a ~300-fold decrease in the equilibrium constant for the binding of dioxygen. This is determined mainly by the ready homolysis of the oxygen adduct of the ligand-methylated complex, $L^2CoO_2^{2+}$ ($k_{-(1\text{-}2)} = 1.66 \times 10^4\ s^{-1}$). Also, the rate constant for oxygen uptake by $L^2Co^{2+}$, $k_{1\text{-}2} = 5.0 \times 10^6\ M^{-1}\ s^{-1}$, is smaller than the rate constants for the capture of akyl radicals by the same complex, $k = (3\text{-}5) \times 10^7\ M^{-1}\ s^{-1}$.[16] The low affinity for oxygen thus seems to be reflected, although to a lesser extent, in the kinetics of the forward reaction as well.

The macrocycle-bound methyl groups exert both steric and electronic influence on the equilibrium constant $K_{1\text{-}2}$. There is little doubt that sterically the methyl groups will hinder the binding of oxygen. Since the reaction involves at least partial electron transfer to oxygen, the reduction potentials of the $Co^{III/II}$ couples, 0.42 V for $L^1Co^{3+/2+}$ [9] and 0.59 V for $L^2Co^{3+/2+}$,[44] work in the same direction. The potential of the ligand-methylated complex is higher than that of $L^1Co^{3+/2+}$, implying that the effect of methylation is again primarily a steric one and that $LCo^{3+}$ is more destabilized relative to $LCo^{2+}$ in the sterically more congested complex. The crystal structure data are not available to find out whether the congestion around the cobalt in $L^2Co^{3+}$ is severe enough to cause an elongation of the axial Co–$OH_2$ bonds, in which case the axial bond-length changes would be expected to be smaller upon reduction of $L^2Co^{3+}$ than $L^1Co^{3+}$.

The equilibrium constant $K_2$ has also decreased drastically from $8.6 \times 10^5\ M^{-1}$ (L = $L^1$) to $<10^3\ M^{-1}$ (L = $L^2$). The latter estimate is based on the assumption that the conversion of <10% of total $L^2CoO_2^{2+}$ (typically 50 μM) to $(L^2Co)_2O_2^{4+}$ would have caused an observable absorbance change at 360 nm in <1 s. The effect of ligand methylation on the value of $K_2$ is probably a cumulative one. Molecular models show that the approach of $L^2Co^{2+}$ to the terminal oxygen of $L^2CoO_2^{2+}$ is made difficult by the macrocycle-bound methyl groups, at least for some orientations. In addition, the higher reduction potential of $L^2Co^{3+/2+}$ relative to $L^1Co^{3+/2+}$ will also result in a smaller value of $K_2$ for the formation of $(L^2Co)_2O_2^{4+}$.

The size of the effect of ligand methylation on the equilibrium constants becomes quite apparent if one compares the composition of oxygen-saturated 0.1 mM solutions of the two cobalt complexes. For L = $L^1$, 60% of the cobalt is present as $L^1CoO_2^{2+}$ and 40% as $(L^1Co)_2O_2^{4+}$; less than 0.5% contains no oxygen. For L = $L^2$, 28% is present as $L^2CoO_2^{2+}$, and 72% does not contain oxygen. The reaction of $L^2Co^{2+}$ with $O_2$ is fully described by eq 1, and the binuclear peroxo complex is not formed to a measurable extent. This makes the $L^2Co^{2+}$ a clean oxygen carrier on short time scales (minutes). At longer times both $L^1Co^{2+}$ and $L^2Co^{2+}$ are irreversibly oxidized by oxygen.

It has been noticed earlier[6,9] that reaction 15 has an unusually high equilibrium constant of $5 \times 10^{13}\ M^{-1}$. This value was

$$L^1Co^{3+} + O_2^- \rightleftharpoons L^1CoO_2^{2+} \qquad (15)$$

calculated from the equilibrium constant $K_{1\text{-}1}$ and the reduction potentials for the couples $O_2/O_2^-$ and $L^1Co^{3+/2+}$. Although our new value for $k_{1\text{-}1}$ changes $K_{1\text{-}1}$ to $2 \times 10^5\ M^{-1}$ and $K_{15}$ to $1 \times 10^{15}\ M^{-1}$, this does not change the original argument, except perhaps to reinforce it. We note that a very similar situation occurs for $L^2Co^{3+}$ as well. The equilibrium constant for the reaction $L^2Co^{3+} + O_2^- \rightleftharpoons L^2CoO_2^{2+}$ has a value of $2 \times 10^{15}\ M^{-1}$, implying that this complex is also strongly stabilized by charge transfer.[6]

**Acknowledgment**. This work was supported by the U.S. Department of Energy, Chemical Sciences Division, under Contract W-7405-Eng-82. We are grateful to Dr. S. Lee for the synthesis of the macrocyclic ligand and to Dr. V. Rutar for his help with the ESR experiments.

(43) Kirker, G. W.; Bakac, A.; Espenson, J. H. *J. Am. Chem. Soc.* **1982**, *104*, 1249.
(44) Liteplo, M. P.; Endicott, J. F. *Inorg. Chem.* **1971**, *10*, 1420.

# Synthesis of Porous Quantum-Size CdS Membranes: Photoluminescence Phase Shift and Demodulation Measurements

**Lubomir Spanhel* and Marc A. Anderson**

*Contribution from the Water Chemistry Program, University of Wisconsin, Madison, Wisconsin 53706.* *Received August 18, 1989*

**Abstract:** Optically transparent CdS membranes have been synthesized. Colloidal Q-CdS particles (particle diameter $d_p$ < 40 Å) carrying short phosphate chains and excess $Cd^{2+}$ ions have been directly converted into a microporous membrane form. By controlling ionic strength and particle concentrations, one can link self-organized fusion-free aggregates and avoid formation of powder-like flocculation products. The resultant unsupported membranes exhibit different mechanical properties (e.g., rigidity, delayed elasticity, and solubility) in the presence of water depending upon the preparation method employed. The membrane form of CdS has distinctively different photophysical properties than the precursor colloidal form. Conversion of weakly red luminescent colloids (broad band at 700 nm) into membranes activated an intense room temperature band edge luminescence (BEL) (narrow bands between 450 and 500 nm) attributed to the recombination of excitons and/or shallowly trapped electron/hole pairs. A specific solvent effect has been observed indicating the major role of water and the related acid–base chemistry in producing radiationless recombination centers at the particle surface. In membrane/solvent experiments, water was found to be a very efficient quencher of the emission while alcohols and acetonitrile did not induce any changes in luminescence properties. A novel Multi-Harmonic Fourier Transform (MHFT) technique was used to determine the average lifetimes of the BEL decay process (≈10 ns in the colloidal form and ≈70 ns in the corresponding membrane form). Simultaneously detected (multiple-frequency domain) phase/modulation data have been used to describe the complex BEL decay, and a three-exponential law best fits the data.

Several recent reports have characterized the photocatalytic and optical properties of large surface area semiconductors.[1-6] One of the main findings is that in polymolecular dispersed metal chalcogenides and metal oxides these properties depend on particle size. Such materials are referred to as Q-materials (Q: showing quantum mechanical effect of exciton confinement).[7] A char-

* Author to whom correspondence should be addressed.

(1) Frank, S. N.; Bard, A. J. *J. Phys. Chem.* **1977**, *81*, 1484.
(2) Kraeutler, B.; Bard, A. J. *J. Am. Chem. Soc.* **1977**, *99*, 7729.
(3) Darwent, J. R.; Porter, G. *J. Chem. Soc., Chem. Commun.* **1981**, 145.

0002-7863/90/1512-2278$02.50/0 

acteristic difference between the Q-state and the bulk state in a semiconductor is an increase in the band gap energy with decreasing particle size. This increase leads to hypsochromic shifts in optical absorption and luminescence spectra. For CdS colloids both the optical absorption threshold and corresponding band edge luminescence (at ≈510 nm)[8] appear to be shifted to shorter wavelengths when the particle size becomes smaller than 6 nm,[9] the characteristic diameter of an exciton in a bulk crystallite.[10] This quantum-size regime in CdS has been widely explored.

Several different environments (glasses,[11] water,[12] alcohols,[13] acetonitrile,[14] reversed micelles,[15] vesicles,[16] and polymers[17]) have been used in studies of not only the growth of CdS particles but also their photophysics and photocatalytic properties. More recently, the use of yeast cells,[18] radiolytically induced growth,[19] and percolative formation of CdS superclusters in zeolites[20] have been reported, suggesting better control over uniformity and particle-size distribution within the quantum-size range.

Particle-size and distribution effects are also of significant importance in sol-gel chemistry,[21] e.g., in the preparation of metal oxides such as $SiO_2$, $Al_2O_3$, and $TiO_2$.[22] Gelation in colloids consolidates or produces organized particle-aggregates. Drying of gels leads to compact and highly uniform porous materials rather than to powder-like products.[23] Better control over particle sizes and the distribution thereof would permit one to tailor not only the optics of a semiconductor device for scientific applications but also the properties of inorganic photocatalysts and ultrafiltration membranes.[24] This paper focuses on the synthesis of

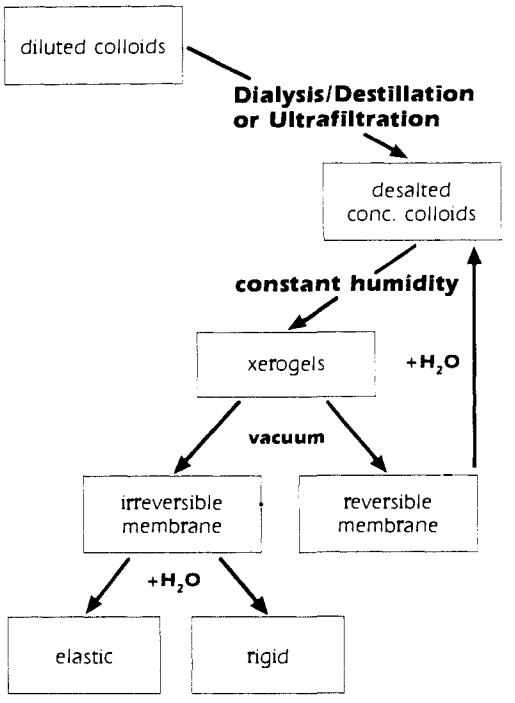


**Figure 1.** Schematic diagram for preparation of CdS membranes with different mechanical properties.

Q-CdS membranes as one possible approach to converting colloidal Q-particles into a membrane. The photoluminescence changes accompanying this transition, including solvent effects, are treated in qualitative form. The results of multiple-frequency phase/modulation measurements to determine photoluminescence lifetimes are also presented.

## Experimental Section

**Apparatus.** Steady-state photoluminescence measurements were performed with a SLM 500C and a Shimadzu RF5000 spectrofluorometer. Spectra from both membranes and concentrated colloids were recorded with use of variable angle front surface accessories. All excitation spectra have been corrected by using Rhodamine B as a quantum counter or dispersion of the monochromatic excitation beam directly to the reference PMT. UV-vis measurements were made with a Varian DMS-80 spectrophotometer. Spectra from colloidal suspensions were obtained from samples contained in 1-cm quartz cells.

Multiple frequency phase/modulation measurements were made with a SLM 48000 MHF (Multi Harmonic Fourier)-fluorometer, located at SLM Instruments in Urbana, IL. A LICONIX (Sunnyvale, CA) Model 4240 NB He-Cd CW laser (excitation at 442 nm) was used as the input source to the harmonic modulator (retroreflecting double KDP crystal Pockel's cell combined with a harmonic comb generator). The duty cycle was approximately 1.5%. For the 4.3-MHz repetition rate the puls duration is ~3.5 ns. The overall power input (per pulse) on sample was 3.5 mW (1 $mm^2$ spot size). This fluorometer permits one to collect simultaneously phase/modulation data at millisecond rates and to resolve lifetimes in the tens of picoseconds.

**Synthesis.** Fabrication of Q-CdS membranes took place in three major steps: (1) preparation of dilute suspensions of Q-particles; (2) concentration of these suspensions under controlled ionic strength conditions; (3) controlled evaporation of solvent from the concentrated colloidal suspensions at room temperature under constant humidity conditions.

**(1) CdS Colloids.** Optically transparent Q-CdS colloids were prepared in a three-neckflask at room temperature. The flask was equipped with a pH electrode for monitoring pH changes during precipitation, with a septum for injection of NaOH or $HClO_4$ for pH adjustment and with a gas inlet dispersion tube for introduction of a $H_2S$-$N_2$ gas mixture. $Cd(ClO_4)_2$ (0.2 M) (from Alfa), 0.1 M sodium polyphosphate (PP) as stabilizer (from Sigma, F.W. = 1592 g/mol, corresponding to 15 $PO_3$ units), and 0.5 M NaOH (from Aesar) were used as stock solutions. $H_2S$ (98%) and $N_2$ (99.9%) gases were used without further purification. Three different initial conditions were employed in making up the

(4) Gratzel, M. *Energy Resources Through Photochemistry and Catalysis*; Academic: New York, 1983.
(5) Fox, M. A., Ed. *Organic Phototransformations in Nonhomogeneous Media*; ACS Symp. No. 278; American Chemical Society: Washington, DC, 1985.
(6) Norris, J. R., Jr., Meisel, D., Eds. *Photochemical Energy Conversion*; Elsevier: New York, 1988; Proceedings of the 7th International Conference on Photochemical Conversion and Storage of Solar Energy.
(7) Henglein, A. *Top. Curr. Chem.* **1988**, *143*, 115–180 and references therein.
(8) (a) Ramsden, J. J.; Gratzel, M. *J. Chem. Soc. Faraday Trans. 1* **1984**, *80*, 919. (b) Ramsden, J. J.; Webber, S. E.; Gratzel, M. *J. Phys. Chem.* **1985**, *89*, 2740–2743.
(9) Spanhel, L.; Haase, M.; Weller, H.; Henglein, A. *J. Am. Chem. Soc.* **1987**, *109*, 5649 and references therein.
(10) (a) Brus, L. E. *J. Chem. Phys.* **1983**, *79*, 5566–5571. (b) *Ibid.* **1984**, *80*, 4403–4409; (c) *Ibid.* **1986**, *108*, 375–378.
(11) (a) Efros, Al. L.; Efros, A. L. *Sov. Phys.-Semicond.* **1982**, *16*, 772. (b) Ekimov, A. I.; Efros, Al. L.; Onushchenko, A. A. *Solid State Commun.* **1985**, *56*, 921.
(12) (a) Fojtik, A.; Weller, H.; Koch, U.; Henglein, A. *Ber. Bunsen-Ges. Phys. Chem.* **1984**, *88*, 969. (b) Baral, S.; Fojtik, A.; Weller, H.; Henglein, A. *J. Am. Chem. Soc.* **1986**, *108*, 375. (c) Kumar, A.; Janata, E.; Henglein, A. *J. Phys. Chem.* **1988**, *92*, 2587.
(13) Chestnoy, H.; Harris, T. D.; Hull, R.; Brus, L. E. *J. Phys. Chem.* **1986**, *90*, 3393–3399.
(14) (a) Kamat, P. V.; Dimitrijevic, N. M.; Fessenden, R. W. *J. Phys. Chem.* **1987**, *91*, 396–401. (b) Kamat, P. V.; Ebbesen, T. W.; Dimitrijevic, N. M.; Nozik, A. *J. Chem. Phys. Lett.* **1989**, *157*, 384–389.
(15) (a) Lianos, P.; Thomas, J. K. *Chem. Phys. Lett.* **1986**, *125*, 299. (b) Dannhauser, T.; O'Neil, M.; Johansson, K.; Whitten, D.; McLendon, G. *J. Phys. Chem.* **1986**, *90*, 6074.
(16) (a) Watzke, H. J.; Fendler, J. H. *J. Phys. Chem.* **1987**, *91*, 854–861. (b) Youn, H. Ch.; Baral, S.; Fendler, J. H. *J. Phys. Chem.* **1988**, *92*, 6320–6327.
(17) Wang, Y.; Mahler, W. *Opt. Commun.* **1987**, *61*, 232.
(18) Dameron, C. T. et al. *Nature* **1989**, *338*, 596.
(19) Hayes, D.; Micic, O. I.; Nenadovic, M. T.; Swayambunathan, V.; Meisel, D. *J. Phys. Chem.* **1989**, *93*, 4603–4608.
(20) (a) Tamura, K.; Hosokawa, S.; Endo, H.; Yamasaki, S.; Oyanagi, H. *J. Phys. Soc. Jpn.* **1986**, *55*, 528. (b) Wang, Y.; Herron, N. *J. Phys. Chem.* **1988**, *92*, 4988–4994. (c) Herron, N.; Wang, Y.; Eddy, M. M.; Stucky, G. D.; Cox, D. E.; Moller, K.; Bein, T. *J. Am. Chem. Soc.* **1989**, *111*, 530–40. (d) Liu, X.; Thomas, J. K. *Langmuir* **1989**, *5*, 57–66.
(21) Klein, L. C.; Garvey, G. J. *Better Ceramics Through Chemistry*; Elsevier: New York, 1984.
(22) See for example: (a) Larbot, A.; Alary, J. A.; Fabre, J. P.; Cuizard, C.; Cot, L. *Mater. Res. Soc. Symp. Proc.* **1986**, *73*, 659–664 and references therein. (b) Fukasawa, J. I.; Tsujii, K. *J. Colloid Interface Sci.* **1988**, *125*, 155–161. (c) Anderson, M. A.; Gieselmann, M. J.; Xu, Q. *J. Membr. Sci.* **1988**, *39*, 243–258. (d) Gieselmann, M. J.; Anderson, M. A.; Moosemiller, M. D.; Hill, C. G., Jr. *Sep. Sci. Technol.* **1988**, *23*(12&13), 1695–1714.
(23) Haas, P. A. *Chem. Eng. Progr.* **1989**, 44–52.
(24) Klein, L. C., Ed. *Sol-Gel Technology for thin Films, Fibers, Preforms, Electronics, and speciality shapes*; Noyes Publications: Park Ridge, NJ, 1988.

aqueous colloids: for A colloids, $1 \times 10^{-4}$ M PP, $3 \times 10^{-4}$ M $Cd^{2+}$, $2 \times 10^{-4}$ M $H_2S$; for B colloids, $8 \times 10^{-5}$ M PP, $12 \times 10^{-4}$ M $Cd^{2+}$, $8 \times 10^{-4}$ M $H_2S$; for C colloids, $3 \times 10^{-4}$ M PP, $4 \times 10^{-4}$ M $Cd^{2+}$, $2 \times 10^{-4}$ M $H_2S$.

Each of the initial colloidal suspensions was made as follows: one liter of Millipore water containing $Cd^{2+}$ and PP was bubbled with nitrogen for 25 min. The pH of the solution was adjusted to 8.8–9.2 with NaOH. The $H_2S$ gas was injected into the nitrogen stream (lowest possible flow rate) over a period of 30 min while the solution was vigorously stirred with a magnetic stirring bar. During this time, NaOH was also added dropwise to keep the pH close to 8.5. The resulting colloid was subsequently purged with a stream of nitrogen gas for 30 min.

**(2) Colloid Desalting and Concentrating.** A 1-L quantity of the fresh colloidal CdS was concentrated by a factor of 5 in a rotary evaporator (12 Torr, 20 °C). The resultant 200 mL of colloidal suspension (pH 7) was placed into a cleaned, molecularly porous dialysis tube (regenerated natural cellulose from Spectra/Por, molecular weight cutoff 3500) and dialyzed against Millipore water. The conductivity of the colloid was checked occasionally during dialysis. The final conductivity of the purified colloid did not exceed 200 $\mu$S. Subsequently, the solution was concentrated by roto-evaporation until the colloidal volume was reduced to 5 mL. The resulting colloidal solution was optically transparent and stable for days against flocculation and particle growth.

**(3) Preparation of Membranes.** A solution containing 5 mL of the concentrated and purified colloid was spread over a flat commercial glass plate (2 × 2 cm) or a plastic Petri dish. These solutions were then kept in a Plexiglas box under 60% relative humidity. After 2 days, an unsupported optically transparent "xerogel" was obtained. Subsequently, the humidity was lowered to 20–30% (humidity present in our own laboratory) over a 6-h period. This reduction is necessary to avoid formation of cracks in the xerogel when it is removed from the box. In the last step, the "xerogel" was converted into a crack-free membrane by drying in a vacuum ($\approx 10^{-3}$ Torr) at 30–40 °C for 2 h. This last step did not induce any mechanical or optical changes. Measurements with an optical microscope indicated that the thickness of these membranes was $\approx 30 \pm 5$ $\mu$m.

## Results and Discussion

**Mechanical Properties of CdS Membranes.** Unsupported Q-CdS membranes prepared by different methods exhibit different mechanical properties. Since these properties are a direct consequence of the preparation conditions employed, we first focus on these conditions in detail.

The procedures for producing compact membranes, in which Q-particles are brought together in close proximity, are summarized in Figure 1. In order to avoid the flocculation of colloids during the transition from a highly dilute state into a superconcentrated xerogel state, controlled procedures for concentration and desalting are required. The use of highly charged polyphosphate (PP) chains ($\approx 15$ $PO_3^-$ units) in the preparations of the initial CdS colloids leads to concentrated desalted sols that are stabilized both electrostatically and sterically. Such sols are kinetically stable for weeks as indicated by the fact that no changes are observed in the optical absorption and luminescence spectrum. The self-organized, slow growth of xerogels taking place at constant humidity was accompanied by a drastic increase in sol viscosity (gelation). It occurs under conditions where interactions in the assemblage of particles and chains cannot be neglected. The resulting xerogels were flat plate-like bodies sometimes able to shrink in the presence of water. Such shrinkage provides evidence of porosity and/or capillarity.

CdS membranes dryed under vacuum showed different types of mechanical behavior. Samples prepared from diluted A colloids (see Experimental Section) shrunk and could be completely transformed back into their colloidal form. B colloids gave rigid irreversible membranes. Membranes prepared from C colloids displayed elasticity in the presence of water. After a few minutes these membranes were flexible in weakly agitated solutions without falling apart.

What are the architecture and the nature of the forces responsible for the different mechanical properties of these membranes? The *chemical* composition of initially prepared diluted colloids seems to contribute, at least in part, to these differences. Let us compare, for example, the rigid with the elastic membranes. For rigid membranes, the lowest possible PP-concentration has been used to keep the starting B colloids stable. Elastic membranes

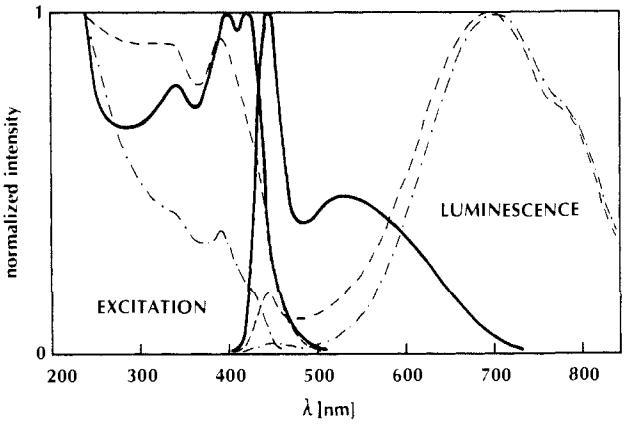


**Figure 2.** Corrected excitation and corrected photoluminescence spectra of small CdS particles in dilute $6 \times 10^{-4}$ M colloidal (- · -), concentrated 0.02 M colloidal (- - -), and water-insoluble membrane (—) form. Excitation spectra normalized at 250 nm (emission wavelength independent). Emission spectra normalized to the scale (excitation wavelength independent). All spectra were taken at room temperature with movable front surface accessories. Initial colloid concentration conditions: $3 \times 10^{-4}$ M PP, $4 \times 10^{-4}$ M $Cd^{2+}$, $2 \times 10^{-4}$ M $H_2S$, $pH_{Start} = 9.0$.

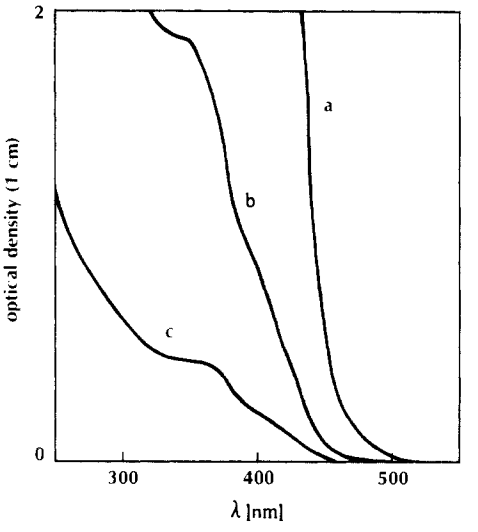


**Figure 3.** Optical absorption spectra (1-cm cell) of small CdS particles under different concentration conditions: (a) 0.02 M, (b) $2.5 \times 10^{-3}$ M, (c) $6 \times 10^{-4}$ M. For initial conditions see Figure 2.

were obtained from C colloids containing by a factor $\approx 4$ higher PP concentration and by factor 4 lower analytical CdS concentration. In all colloids, an excess of $Cd^{2+}$ ions was present. On the other hand, $Cd^{2+}$ ions have not been found in significant amounts in supernatants collected after desalting the starting colloids. It is known from inter-particle electron-transfer studies that $Cd^{2+}$ ions and PP chains play important roles in linking together chemically different semiconductor particles.[25] In terms of these results short- and long-range structures like $(CdS)_p$-Cd-$(CdS)_p$, $(CdS)_p$-PP-$(CdS)_p$, and $(CdS)_p$-PP-Cd-PP-$(CdS)_p$ also seem to be important in producing the membranes with different mechanical properties. In order to better understand the physical characteristics of these materials, small-angle X-ray scattering (SAXS) measurements are now being performed.

**Colloid → Membrane Transition and Corresponding Spectroscopic Changes.** Figure 2 depicts excitation and photoluminescence spectra of small CdS particles in dilute and concentrated "colloidal" forms (dashed and broken lines, respectively) and in the "membrane" form without water (solid line). The concentration dependence of the CdS absorption spectrum is drawn in Figure 3. At low concentrations (spectra b and c) the spectral

(25) Spanhel, L.; Henglein, A.; Weller, H. *Ber. Bunsenges. Phys. Chem.* **1987**, *91*, 1359–1363; *J. Am. Chem. Soc.* **1987**, *109*, 6632–6635.

intensity of the two shoulders at 350 and 400 nm increases as the colloid concentration increases. A red-shifted steep absorption band edge with an onset at 510 nm has been observed in the 0.02 M colloid (spectrum a). On the other hand, a pronounced 400-nm peak and two shoulders at 430 and 350 nm are intensified and evident in the excitation spectra of the increasingly concentrated colloid (see Figure 2). These features can be attributed to exciton-like transitions in relatively strongly quantized particles. The average crystallite size in the presented colloids and membranes was calculated from X-ray powder diffraction data to be about 40 Å. This average size estimate also can be obtained from the correlation shown in Figure 15 of ref 9 by taking 450 nm as the excitation threshold from Figure 2. The spectroscopic observation described above can be related to noticeable particle aggregation in increasingly concentrated colloids, thus explaining the tendency to approach the optical absorption spectrum of bulk CdS (absorption onset at 550 nm).

The fact that excitonic transitions are less pronounced or not observable in UV–vis spectra clearly shows that not all intrinsic absorption processes in CdS produce luminescence. Direct excitations into the excitonic states are favored with respect to the emission of luminescence light. Electronic transitions into the continuum (above the transition into the lowest excitonic state) may induce rapid relaxations (for example back into the lowest excitonic state), coupling to vibrations, and other related nonradiative processes. Such processes could explain the observed differences in the absorption and excitation spectra of the colloids. As can be seen, concentration increases did not substantially alter the emission spectrum of these colloids. Their spectra contain a less intense BEL band at 450 nm and a more intense broad band which is strongly shifted to ≈700 nm. These spectra indicate that, after light absorption in the colloids, the photogenerated $e^-/h^+$ pairs are deeply trapped, emitting red (≈700 nm) light upon their recombination. Only a small fraction of excitons (or weakly trapped $e^-/h^+$ pairs) produce 450-nm photons, i.e., without apparent Stokes shift. The quantum efficiency of luminescence is low (<1%) for both of these colloids as is generally observed in colloidal semiconductors at room temperature. Faster nonradiative recombination processes predominate and determine the lifetime of charge carriers in these colloidal systems.

The yellowish, optically transparent CdS membranes give much different spectroscopic results. These porous unsupported materials exhibit bright luminescence at room temperature. The quantum yield of the luminescence has been determined (using 400 nm as the excitation wavelength and assuming 100% optical absorption at this wavelength) to be 25%, 80 times higher when compared to their concentrated precursor colloids. These membranes are characterized by a new spectrum of emitting states (Figure 2). The 700-nm band is missing and radiative processes close to the band edge are now activated. The exciton peaks in the excitation spectrum are more pronounced and more intense at longer wavelengths. Surprisingly, the frequencies characteristic of the excitonic states, now producing mainly a bright blue emission (450 nm) and a less intense green-yellow emission (≈520 nm), did not change. This result implies that under even the extreme concentration conditions employed, very small clusters tend to aggregate rather than to fuse together. The latter process would produce larger particles and would result in a red shift in both the optical and BEL-emission spectra. The spectroscopic picture of this membrane as a whole indicates the dominance of electron-hole recombination near the band edge irrespective of the excitation wavelength. The spectra in Figure 4 indicate that similar recombination processes are observed in a membrane obtained from a slightly different colloidal preparation. Unlike the previous sample, only one transition (at ≈460 nm) is seen in the excitation spectrum. (A corresponding difference has been found in the UV–vis spectra of the two membranes. The sample from Figure 2 has shown two weak shoulders at 440 and 400 nm while the sample from Figure 4 has only one at 470 nm, which coincides with the observed peaks in the excitation spectra.) This membrane is composed of slightly larger particles (BEL-emission maximum at ≈480 nm), but they are still smaller than the bulk

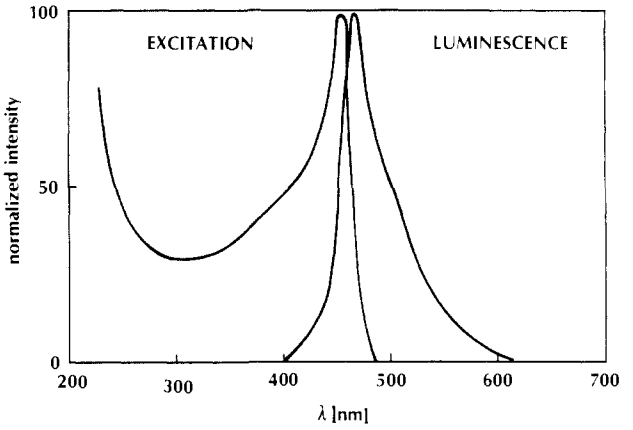


**Figure 4.** Corrected excitation spectra (emission wavelength independent) and corrected emission spectra (excitation wavelength independent) of an irreversible membrane obtained from following starting colloid preparation conditions: $8 \times 10^{-5}$ M PP, $12 \times 10^{-4}$ M $Cd^{2+}$, $8 \times 10^{-4}$ M $H_2S$, pH = 8.8; for experiment conditions see Figure 2.

crystal-like 60-Å particles characterized by a green band edge emission at 510 nm.

The question remains as to why the membrane spectra shown in Figure 2 are structured while those in Figure 4 are not? Recent studies on CdSe[26a,b] and CdS[18] clusters provide evidence that the electronic structure of these quantum materials consists of a single HOMO–LUMO peak (1S–1S transition) and a continuum absorption at higher energies. Conclusions drawn from these studies would indicate that transitions into the lowest and higher excitonic states[26c] cannot explain the structured excitation spectrum in Figure 2. The CdS membrane characterized in Figure 2 seems to have a broader size range dominated by magic particle sizes.[7] Its excitation spectrum suggests two HOMO–LUMO peaks (at 350 and 400 nm) of the smaller particles hidden in continuum of the largest group of particles, characterized by the HOMO–LUMO transition at 430 nm. On the other hand the membrane characterized by the spectrum in Figure 4 shows just one pronounced HOMO–LUMO transition indicating a narrower size range. A different size distribution might explain different shapes of the emission spectra of the two membranes as well. It has been reported already that relatively narrow BEL bands, such as those seen in Figure 4, can be observed only in those Q-CdS colloids that have a relatively narrow size distribution.[9] Broader size ranges give broader emission shapes such as the one shown in Figure 2.

Nevertheless, processes that could occur in particle aggregates cannot be neglected in these materials. Account should be taken of mutual interactions between connected Q-particles (differently sized) within the photoexcited membrane. Due to different Q-sizes, i.e., due to different band gaps, there might exist driving forces for interparticle exciton transfer. Consider a broad size range as suggested for the membrane in Figure 2. An excitation at 350 nm would generate electrons and holes in all particles whose HOMO–LUMO transition is lower in energy than 350 nm. Subsequently, those electrons and holes produced in smaller particles (with larger band gap) could relax into larger particles (with smaller band gap) recombining there in either radiative or nonradiative processes. This could explain why both 350- and 400-nm excitation transitions gave the same emission spectrum. At present, we are engaged in transmission electron microscopic studies in order to determine the physical characteristics of these membranes.

When comparing the luminescence spectra of the water free membranes with their colloidal precursors, one should note that the membranes are characterized by (1) blue shift and a narrowing

(26) (a) Alivisatos, A. P.; Harris, A. L.; Levinos, N. J.; Steigerwald, M. L.; Brus, L. E. *J. Chem. Phys.* **1988**, *89*, 4001–4011. (b) Steigerwald, M. L.; Alivisatos, A. P.; Gibson, T. D.; Harris, T. D.; Kortan, R.; Muller, A. J.; Thayer, A. M.; Duncan, T. M.; Douglass, D. C.; Brus, L. E. *J. Am. Chem. Soc.* **1988**, *110*, 3046–3050. (c) Ekimov, A. I.; Onushchenko, A. A. *Pis'ma Zh. Eksp. Teor. Fiz.* **1984**, *40*, 337.

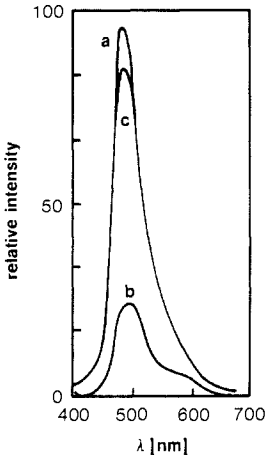


**Figure 5.** Reversible luminescence quenching in Q-CdS membrane in presence of water. The same membrane sample as employed in Figure 4 was used: (a) initial spectrum under ambient laboratory conditions and (b) after wetting with water, and (c) recovered spectrum after subsequent drying.

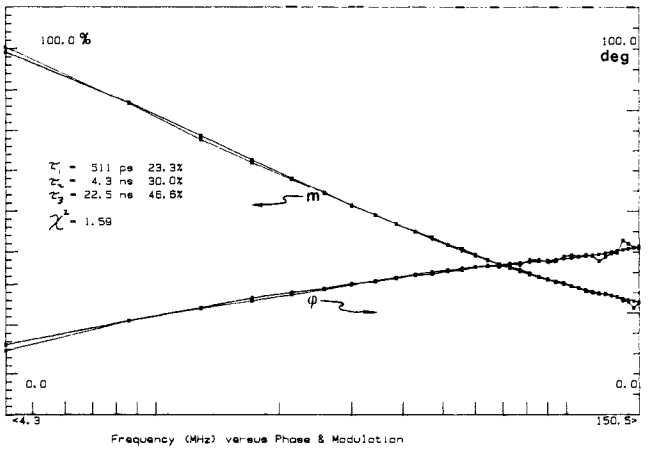


**Figure 6.** Phase shift $\phi$ (in deg) and demodulation $m$ (in %) of the BEL-emission band (at 460 nm) in 0.02 M Q-CdS colloid as a function of modulation frequency. Three lifetime component analysis of the data with corresponding reduced $\chi^2$ ($\chi^2$, a numerical value reflecting the overall goodness of fitting); $\lambda_{ex}$ = 442 nm. The photoluminescence spectrum of this colloid sample is shown in Figure 2.

in the spectrum of emitting states and (2) elimination of deep surface trapping sites with a corresponding increase in the intensity of the BEL. One should remember that the change from the colloid to the membrane involves both particle consolidation and removal of water from the environment of the particle. The particle size dependence of the band gap, the chemical nature of surface traps (i.e., the environment) and the particle size distribution are the factors determining the intensity and spectral distribution of emitting states. For example, alkylamines and thioorganics,[15b] high alcohol content, or cadmium hydroxide coatings[27] can be used as surface modifiers to enhance the luminescence intensity in aqueous colloids at ambient temperature. Additionally, as noted above, a blue shift in the emission spectrum and an increase in the intensity of luminescence has been achieved with use of the mentioned surface modifiers. These results lead one to conclude that the photoluminescence spectra of CdS membranes in an ambient air environment have intensities and spectral distributions comparable to those of spectra obtained from chemically modified colloidal precursors in an aqueous environment. The role of water and the related acid–base chemistry in the observed photoluminescence changes are discussed below.

**Establishment of the Membrane/Liquid Interface.** Several membrane/liquid experiments have been performed in efforts to elucidate the previously[9,15b,27] predicted roles of the water molecules and SH groups in producing surface traps that are responsible for radiationless recombination processes. Water is a very efficient quencher of the band edge photoluminescence in CdS membranes. Figure 5 shows the initial spectrum (a) of an irreversible CdS membrane used in these experiments. After the membrane was wet with a small amount of water, the luminescence intensity dropped as shown in spectrum b. Spectrum c reflects a recovery of the quenched luminescence after subsequent drying without changing the geometric position of the membrane in the spectrofluorometer. The presence of water within the pore structure of the membrane decreases the ability of the CdS to luminesce. A treatment of this hydrated membrane with alcohols or acetonitrile accelerates the recovery of the luminescence spectrum. It has the same effect as the drying. However, when alcohols and acetonitrile replace the ambient air within the pores, no changes in luminescence intensity occur. This result is unlike that observed for aqueous colloids where an increase in the luminescence intensity occurs. These results indicate it is not a general solvent effect responsible for the observed quenching but rather a specific $H_2O$ via $H^+/OH^-$ related effect. For example, protonation of surface sulfur groups and/or their association with water molecules could produce different local environments within which photogenerated holes (chemically $S^{\bullet-}$) could appear. Such SH groups and/or more complex association products could act as different types of traps for photogenerated holes and cause their radiationless recombination with photogenerated electrons. As to whether the quenching is static or dynamic, the chemical nature of surface sites and the corresponding mechanism causing the radiationless recombinations cannot be exactly given. It is interesting to note that neither dried nor hydrated CdS membranes containing excess $Cd^{2+}$ ions give emission spectra containing the 700-nm luminescence band whereas their colloidal counterparts do (see Figure 2). It is believed that "sulfur vacancies" act as orange-red luminescence centers as this broad 700-nm band becomes more intense with increasing $Cd^{2+}$ or acetonitrile content, respectively.[8,28] Hence, it was not unexpected that an addition of water to the membrane did not recover this 700-nm band. However, subsequent addition of an alcoholic or aqueous $Cd^{2+}$ solution (or acetonitrile) did not activate the orange-red centers. At present it is difficult to explain why the "sulfur vacancies" act as orange-red luminescence centers in colloidal CdS but do not act in this fashion in microporous CdS membranes. A detailed spectroscopic study, including effects of thickness, pore size, and different solid/liquid interfaces with supported and unsupported Q-CdS membranes, will be the subject of forthcoming papers.

**Q-CdS Photoluminescence under Modulated Multiple-Frequency Laser Excitation.** There are very few reports in the literature concerning the application of phase/modulation fluorescence spectroscopy in semiconductor surface research.[29,30] Blanc and Curie used modulated photoexcitation in stationary luminescence phase shift measurements at various temperatures to determine trap characteristics in doped ZnS and CdS macrocrystallites. In our study, a phase coherent pulse modulated laser excitation has been applied in phase/modulation measurements in order to determine the decay characteristics and the lifetime of Q-CdS photoluminescence. In this dynamic frequency-domain spectroscopy the pulse modulated laser light contains a comb of harmonic frequencies ($\nu$, $2\nu$, $3\nu$, ..., 250 MHz). The photoexcited sample is forced to emit luminescence light at the same frequencies. Because of the finite lifetime of the excited states, the modulated emission is delayed in phase by an angle $\phi$ and has smaller amplitude $m$ (i.e., is less modulated) relative to the excitation. Except for time-domain spectroscopy, $m$ and $\phi$ are measured values that can be used to calculate the lifetime of fluorescence. The desired frequency range and the number of modulation frequencies within this range determine the range and number of measurable $m$ and $\phi$ values and thus the accuracy of the lifetime determination.

(27) Spanhel, L.; Weller, H.; Fojtik, A.; Henglein, A. *Ber. Bunsenges. Phys. Chem.* **1987**, *91*, 88–94.

(28) Henglein, A. *Ber. Bunsenges. Phys. Chem.* **1982**, *86*, 301–305.
(29) Blanc, G.; Ceva, T. *J. Lumin.* **1973**, *6*, 147–166.
(30) Blanc, G.; Curie, D. *J. Lumin.* **1985**, *34*, 125–132.

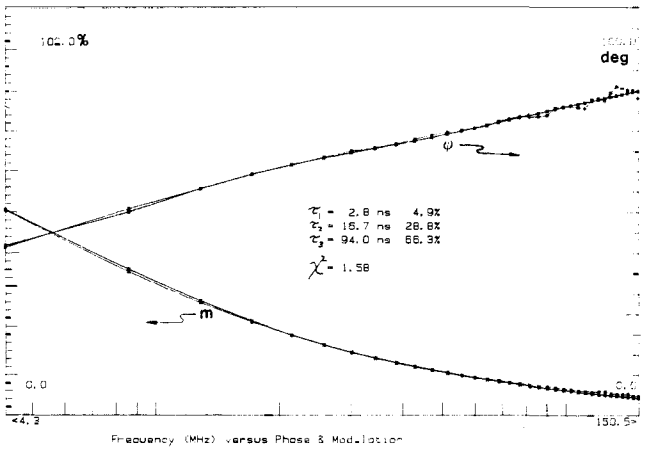


**Figure 7.** $\phi/m$ and calculated lifetime data from the same Q-CdS membrane sample as shown in Figure 2. Excitation and detection conditions as in Figure 6.

Details of this method are described by Lakowicz[31] and Demas.[32]

The $m$ and $\phi$ data for the band edge luminescence in 0.02 M Q-CdS colloid and in another membrane are shown in Figures 6 and 7 as a function of modulation frequency $\nu$. These samples are those used to generate the spectra in Figure 2. In both cases with increasing $\nu$ the measured $\phi$ increases and $m$ decreases. These results are what one would expect on theoretical grounds, e.g., for a constant lifetime, increasing the modulation frequency should result in larger phase shifts and a greater degree of demodulation.[31] Comparing in Figures 6 and 7, one can also recognize that at any set frequency the luminescence waves produced in the membrane are less modulated and show larger phase shifts than waves produced by the colloid. From these figures and from Figure 2 it becomes evident that the lifetime of photogenerated $e^-/h^+$ pairs producing BEL is longer in the membrane than in its less intensely luminescing colloidal precursor.

The phase/modulation data presented have also been analyzed in terms of multi-exponential decay with a statistical nonlinear least-squares approach[33,34] in which a Fourier transform of the real-time response function

$$I(t) = \sum_i (f_i/\tau_i)e^{-t/\tau_i} \qquad (1)$$

is performed. This approach is unlike the pulse method, which provides a decay curve in real time convolved with a pulse profile of finite width. Three-exponential law analysis gave the best fit (lowest $\chi^2$ values) and resulted in three lifetime components $\tau$ with corresponding fractional contributions $f_i$ as depicted in Figures 6 and 7. The average lifetime $\langle\tau\rangle = \sum f_i\tau_i$ has been calculated to be 12 ns in the colloid. This lifetime is significantly shorter than that calculated for the membrane (67 ns). The shorter average lifetime of the BEL emission in the less intensely luminescing colloid can be understood following the previous time-domain studies with Q-CdS colloids. The fast crossing of photogenerated $e^-/h^+$ pairs into deep traps (with $k_c$ = corresponding rate constant) and predominant nonradiative processes ($k_{nr}$) that compete with radiative band edge transitions ($k_r$) decrease the observed lifetime of BEL $\tau_{obs} = (k_c + k_{nr} + k_r)^{-1}$ due to $k_{nr} \approx k_c \gg k_r$. Unlike the colloidal system, the crossing into deep traps within the photoexcited membrane does not occur because of their absence (see Figure 2), and radiative recombinations close to the band edge are more frequent. Moreover, the relatively long average lifetime of 67 ns in the membrane suggests that the initial crossing into shallow traps with subsequent radiative recombinations is more frequent than direct exciton recombinations in Q-CdS particles.

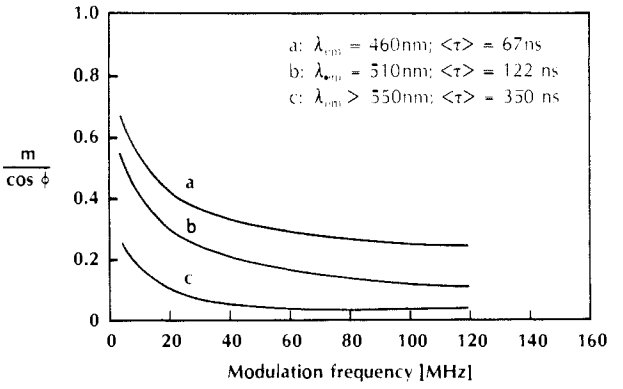


**Figure 8.** Investigation of the membrane sample from Figure 7 at different emission wavelengths. $m/\cos\phi$ ratio as a function of modulation frequency and photoluminescence wavelength. The average lifetimes $\langle\tau\rangle$ at 460, 510, and above 550 nm obtained from three-component analysis of $\phi/m$ data, $\lambda_{ex}$ = 442 nm.

Another interesting aspect of this frequency-domain technique is the possibility of studying the nature of the photoluminescence by comparing the phase shift and demodulation data from the same sample. The $m$ and $\phi$ values from the membrane sample in Figure 2 were obtained at 460, 510, and above 550 nm. The result of this experiment is illustrated in Figure 8, which shows the longer average lifetime of $e^-/h^+$ pairs at longer emission wavelengths and the wavelength and frequency dependence of the $m/\cos\phi$ ratio. This ratio is a sensitive indicator of the nature of photoluminescence.[31]

For first-order kinetics, a Fourier transform of the function in eq 1 leads to the phase-lifetime formula

$$\tau_p = \omega^{-1} \tan\phi \qquad (2)$$

and the modulation-lifetime formula

$$\tau_m = \omega^{-1}[(1/m^2) - 1]^{1/2} \qquad (3)$$

where $\omega$ is the circular frequency ($2\pi \times$ modulation frequency in Hz). With eq 2 and 3, it can be shown that for single-exponential decay the ratio $m/\cos\phi = 1$ ($\tau_m = \tau_p = \tau$). Furthermore, observation of $m/\cos\phi > 1$ proves the occurrence of an excited-state reaction whereas $m/\cos\phi < 1$ reflects ground-state heterogeneity or a reverse reaction that is dependent upon the investigated system. As seen in Figure 8, at any one frequency and any wavelength the $m/\cos\phi$ is smaller than 1, indicating complexity, i.e., emission of the luminescence in the membrane from more than one or two electronic states. The photoluminescence in this system seems to result from recombination of differently trapped charge carriers rather than from a photochemical excited-state reaction that produces qualitatively new luminescing products, as recently postulated by Wang and Herron.[20b] These data are in agreement with the trap-recombination theory[7,13] in CdS as they show that with increasing emission wavelength the $m/\cos\phi$ ratio decreases. The photogenerated charge carriers in deeper traps (light emission above 550 nm) live longer than in more shallow traps (light emission at 510 nm) so that they cannot keep up with high modulation frequencies. This explains lower $m/\cos\phi$ ratios at longer wavelengths (for any given modulation frequency) and indicates physical significance of calculated average lifetimes. The $\langle\tau\rangle$ values in Figure 8 are the result of the three-component analysis that gave the lowest numerical $\chi^2$ value at any emission wavelength. Hence, the question arises as to whether the quantities $\tau_i$ and $f_i$ in Figures 6 and 7 may or may not have any physical meaning. Kamat et al.[35] have reported three-component analysis of the 515-nm BEL-emission band from time-domain measure-

(31) Lakowicz, J. R. *Principles of Fluorescence Spectroscopy*; Plenum Press: New York, 1985.
(32) Demas, J. N. *Excited State Lifetime Measurements*; Academic Press: New York, 1983.
(33) Knutson, J. R.; Beechem, J. M.; Brand, L. *Chem. Phys. Lett.* **1983**, *6*, 501–507.
(34) Gratton, E.; Jameson, D. M. *Anal. Chem.* **1985**, *57*, 1694–1697.
(35) Kamat, P. V.; Dimitrijevic, N. M.; Nozik, A. J. *J. Phys. Chem.* **1989**, *93*, 2873–2875; 4259–4263.

ments on colloidal CdS particles in acetonitrile. They associated the three observed lifetimes to "initial weak trapping, electron reemission to the conduction band and radiative recombination from the conduction band after traps are filled". However, many decay curves and, as shown in Figure 8, any series of phase/modulation data could be described fairly well with three components. Additionally, the CdS particles investigated here fall in the polymolecular quantum-size regime (BEL position at 460 nm) while CdS particles in acetonitrile have rather macrocrystalline properties (BEL position at 515 nm). Additional work is needed to prove the significance of the three-component $\phi/m$ decay data.

In summary, this paper provides the first description of the sol-gel based preparation of a compact quantum semiconductor membrane. In this preliminary work we have only attempted to give a general overview of their spectroscopic properties. Additionally, the preliminary results presented here have demonstrated the usefulness of the multiple-frequency phase/modulation approach and shown that this approach is at least comparable to picosecond time-domain techniques. These results also demonstrate that the technique of MHFT spectroscopy might be extended to dynamic semiconductor surface investigations.

**Acknowledgment.** We gratefully acknowledge the financial support by the U.S. EPA (R 813457-01-0) and U.S. DOE (PO#AX079886-1). We thank Dr. Kerry M. Swift from SLM Instruments for obtaining the phase and modulation data and Professor A. B. Ellis and C. G. Hill, Jr., for helpful discussions.

# A Novel Monooxoruthenium(V) Complex Containing a Polydentate Pyridyl Amine Ligand. Syntheses, Reactivities, and X-ray Crystal Structure of $[Ru^{III}(N_4O)(H_2O)](ClO_4)_2$

**Chi-Ming Che,*[1a] Vivian Wing-Wah Yam,[1a,c] and Thomas C. W. Mak[1b,†]**

*Contribution from the Departments of Chemistry, University of Hong Kong, Pokfulam Road, Hong Kong, and The Chinese University of Hong Kong, Shatin, New Territories, Hong Kong.*
*Received September 21, 1988*

**Abstract:** The syntheses and characterization of *cis*-$[Ru^{III}(tepa)Cl_2]^+$, $[Ru^{III}(N_4O)(H_2O)]^{2+}$, and $[Ru^{V}(N_4O)O]^{2+}$ complexes are described [tepa = tris(2-(2-pyridyl)ethyl)amine, $N_4OH$ = bis(2-(2-pyridyl)ethyl)(2-hydroxy-2-(2-pyridyl)ethyl)amine]. The molar magnetic susceptibilities for $[Ru^{III}(N_4O)(H_2O)]^{2+}$ and $[Ru^{V}(N_4O)O]^{2+}$ complexes are 1.79 and 2.2 $\mu_B$, respectively. The X-ray structure of $[Ru^{III}(N_4O)(H_2O)](ClO_4)_2$ has been determined: $[Ru^{III}(C_{21}H_{23}N_4O)(H_2O)](ClO_4)_2$, $M$ = 666.43, monoclinic, space group $P2/c$ (no. 13), $a$ = 11.644 (1) Å, $b$ = 11.937 (3) Å, $c$ = 18.856 (6) Å, $\beta$ = 105.39 (2)°, $V$ = 2527 (1) Å$^3$, $Z$ = 4, $D_x$ = 1.753, $D_c$ = 1.752 g cm$^{-3}$, $\mu$(Mo K$\alpha$) = 8.82 cm$^{-1}$. The Ru-O($OH_2$) and Ru-O($N_4O$) distances are 2.115 (3) and 1.961 (4) Å, respectively. The $[Ru^{V}(N_4O)O]^{2+}$ complex shows an intense Ru=O stretch at 872 cm$^{-1}$ which is absent in the $[Ru^{III}(N_4O)(H_2O)]^{2+}$ complex. The Ru(V) state in $[Ru^{V}(N_4O)O]^{2+}$ has also been confirmed by spectrophotometric redox titration in 0.1 M $HClO_4$ by using $[Ru^{II}(NH_3)_4(bpy)]^{2+}$ (bpy = 2,2'-bipyridine) as the redox titrant. A stoichiometry of 1:3 has been obtained. The cyclic voltammograms of both $[Ru^{III}(N_4O)(H_2O)]^{2+}$ and $[Ru^{V}(N_4O)O]^{2+}$ complexs show two couples at 0.35 and 1.02 V vs SCE in aqueous medium at pH = 1, assignable to a Ru(III/II) and a Ru(V/III) couple, respectively. At 5.5 > pH > 3.5, the wave for the Ru(V/III) couple splits into two waves, a pH-independent one-electron wave for the Ru(V/IV) couple and a two-proton-one-electron wave with a slope of -117 mV/pH unit for the Ru(IV/III) couple. The Ru(IV) state is found to be thermodynamically unstable with respect to disproportionation into Ru(III) and Ru(V) at pH < 3.5. The $[Ru^{V}(N_4O)O]^{2+}$ complex is found to be an active oxidant, capable of oxidizing both activated C-H bonds and the C-H bond of cyclohexane. Studies on the reactions of $[Ru^{V}(N_4O)O]^{2+}$ with organic substrates indicated that the Ru(V)=O has a higher affinity for hydrogen atom/hydride abstraction than oxo-transfer reaction to C=C double bond.

High-valent oxo complexes of ruthenium have long been known to be active oxidants for a variety of substrate oxidation reactions.[2] The interest in studying these complexes stems its origin from the postulation that high-valent oxoiron species is involved in the enzymatic reactions of cytochrome P-450, which is the hemoprotein known to catalyze hydroxylation of unactivated C-H bonds under mild conditions. Ruthenium, being in the same group as iron, is particularly interesting to study owing to the wide applicability of its oxides such as $RuO_4$ in synthetic organic chemistry. Despite the recent progress in successful isolation and characterization of monooxoruthenium(IV) and dioxoruthenium(VI) complexes,[2,3] there are few studies on oxoruthenium(V) species[4,5] which are suggested to be the reactive intermediates in the oxidation of water to oxygen.[6] The monooxoruthenium(V) complexes should deserve special attention since they could provide an insight into the mechanism played by the Ru(V)=O moiety in these reactions. Although a large number of catalytic systems using ruthenium(III) complexes and an oxygen atom donor such as PhIO[7] or NaOCl[8] are known to activate epoxidation of olefins via a postulated "Ru(V)=O" intermediate, attempts to isolate this class of compounds have been unsuccessful.

† Author to whom correspondence on X-ray structure should be sent.

(1) (a) Department of Chemistry, University of Hong Kong, Pokfulam Road, Hong Kong. (b) Department of Chemistry, The Chinese University of Hong Kong, Shatin, New Territories, Hong Kong. (c) Present address: Department of Applied Science, City Polytechnic of Hong Kong, Tat Chee Avenue, Kowloon, Hong Kong.

(2) (a) Roecker, L.; Meyer, T. J. *J. Am. Chem. Soc.* **1987**, *109*, 746. (b) Lau, T. C.; Kochi, J. K. *J. Chem. Soc., Chem. Commun.* **1987**, 798. (c) Griffith, W. P.; Ley, S. V.; Whitcombe, G. P.; White, A. D. *J. Chem. Soc., Chem. Commun.* **1987**, 1625. (d) El-Hendway, A. M.; Griffith, W. P.; Piggott, B.; Williams, D. J. *J. Chem. Soc., Dalton Trans.* **1988**, 1983. (e) Marmion, M. E.; Takeuchi, K. J. *J. Am. Chem. Soc.* **1988**, *110*, 1472. (f) Llobet, A.; Doppelt, P.; Meyer, T. J. *Inorg. Chem.* **1988**, *27*, 514.

(3) (a) Che, C. M.; Wong, K. Y.; Mak, T. C. W. *J. Chem. Soc., Chem. Commun.* **1985**, 546. (b) Mak, T. C. W.; Che, C. M.; Wong, K. Y. *J. Chem. Soc., Chem. Commun.* **1985**, 986. (c) Che, C. M.; Wong, K. Y.; Leung, W. H.; Poon, C. K. *Inorg. Chem.* **1986**, *25*, 345. (d) Che, C. M.; Lai, T. F.; Wong, K. Y. *Inorg. Chem.* **1987**, *26*, 2289. (e) Che, C. M.; Leung, W. H. *J. Chem. Soc., Chem. Commun.* **1987**, 1376.

(4) (a) Wong, K. Y.; Che, C. M.; Anson, F. C. *Inorg. Chem.* **1987**, *26*, 737. (b) Che, C. M.; Wong, K. Y. *J. Chem. Soc., Chem. Commun.* **1986**, 229. (c) Che, C. M.; Wong, K. Y.; Mak, T. C. W. *J. Chem. Soc., Chem. Commun.* **1985**, 988.

0002-7863/90/1512-2284$02.50/0 